Chinese Journal of
POLYMER SCIENCE

ARTICLE

https://doi.org/10.1007/s10118-018-2037-7
Chinese J. Polym. Sci. 2018, 36, 488–496

An Efficient Algorithm for Self-consistent Field Theory Calculations of Complex Self-assembled Structures of Block Copolymer Melts

Jun-Qing Song, Yi-Xin Liu*, and Hong-Dong Zhang

State Key Laboratory of Molecular Engineering of Polymers, Department of Macromolecular Science, Fudan University, Shanghai 200433, China

Abstract Self-consistent field theory (SCFT), as a state-of-the-art technique for studying the self-assembly of block copolymers, is attracting continuous efforts to improve its accuracy and efficiency. Here we present a fourth-order exponential time differencing Runge-Kutta algorithm (ETDRK4) to solve the modified diffusion equation (MDE) which is the most time-consuming part of a SCFT calculation. By making a careful comparison with currently most efficient and popular algorithms, we demonstrate that the ETDRK4 algorithm significantly reduces the number of chain contour steps in solving the MDE, resulting in a boost of the overall computation efficiency, while it shares the same spatial accuracy with other algorithms. In addition, to demonstrate the power of our ETDRK4 algorithm, we apply it to compute the phase boundaries of the bicontinuous gyroid phase in the strong segregation regime and to verify the existence of the triple point of the O^{70} phase, the lamellar phase and the cylindrical phase.

Keywords Block copolymer; Self-consistent field theory; Algorithm; Pseudo-spectral; Phase structure

Citation: Song, J. Q.; Liu, Y. X.; Zhang, H. D. An Efficient Algorithm for Self-consistent Field Theory Calculations of Complex Self-assembled Structures of Block Copolymer Melts. Chinese J. Polym. Sci. 2018, 36(4), 488–496.

INTRODUCTION

The main idea of the polymer self-consistent field theory (SCFT) originated from the work of Edwards[1] on the size of polymers with excluded volume in the middle of 1960s, which was extended by de Gennes[2], Helfand[3], and Hong and Noolandi[4] to the study of inhomogeneous polymers. In recent years, perhaps the most prominent application of the SCFT theory is to study the self-assembly of block copolymers with various topological structures and characteristic properties[5–12]. In general, it is impossible to find analytical solutions for the set of SCFT equations. Therefore, either numerical or analytical approximation approaches are required to solve the SCFT equations. Analytical approximation methods, such as the random phase approximation (RPA)[13] and the strong stretching theory (SST)[14] , only cover a limited range of parameter space due to the introduction of further approximations in addition to the mean field approximation. However, to examine the density distribution of each component and to address the stability of several competing complex microstructures such as the bicontinuous double gyroid phase (G) and the ordered bicontinuous double diamond (OBDD) phase[15], usually requires the solution of the SCFT model where numerical methods play a central role.

With a given updating scheme in a typical numerical SCFT calculation, the most time-consuming procedure is to evaluate the propagators from the modified diffusion equations (MDE)[5]. The propagator describes the probability to find a segment in a polymer chain with contour length s situated at $\mathbf{r}$, which is essential for calculating the density operator and the single chain partition function. In 1994, Matsen and Schick[15] made a major progress in solving SCFT equations efficiently by developing a spectral method. In particular, they expanded the spatial dependence of the unknown functions into a complete set of smooth basis functions, and transferred the calculation from real space into Fourier space. This method works well in evaluating the free energy of presumed phase structures thus allowed them to construct a complete phase diagram of diblock copolymers for the first time. However, the spectral method has an important limitation that it relies on knowing phase structures in advance in order to take advantage of their symmetries to reduce the computational cost. On the other hand, Drolet and Fredrickson[16] proposed a combinatorial screening strategy for exploring new structures of block copolymers by solving SCFT equations in real space. The real-space technique enables one to search for unknown structures by initializing simulations with random field/density configurations. Later, Rasmussen and Kalosakas[17] developed a pseudo-spectral method based on an operator-splitting scheme (OS2), which greatly improves the efficiency of the real-space SCFT calculation. After that the OS2 method has been widely accepted as the method of choice for real-space SCFT calculations.

* Corresponding author: E-mail lyx@fudan.edu.cn
Received July 2, 2017; Accepted September 8, 2017; Published online December 29, 2017

As a second order time-stepping algorithm, the OS2 method leaves room for further improvement. Cochran, Garcia-Cervera and Fredrickson[18] proposed a fourth-order pseudo-spectral algorithm (CGF4) based on a backward differentiation formula for Laplacian operator and an Adams-Bashford formula for the source term to overcome the difficulty in calculations of the gyroid structure in intermediate-to-strong segregation regime. With this algorithm, they determined phase boundaries that enclose the gyroid at χN up to 100. Another 4th-order algorithm (RQM4) was developed by Ranjan, Qin and Morse[19] by simply applying Richardson extrapolation on the OS2 algorithm. The authors claimed that this algorithm is more efficient than the spectral method at a large number of plane waves for calculation of linear response functions. In contrast to the CGF4 method, the RQM4 method does not need a second algorithm to start it up. Apart from these fourth-order pseudo-spectral algorithms, Tong *et al.*[20] developed an efficient real-space algorithm based on the multigrid method.

Recently, Stasiak and Matsen have systematically benchmarked the performance of various pseudo-spectral algorithms[21]. By directly comparing the computation time for reaching a certain accuracy of the free energy of the gyroid and the spherical phases, they concluded that the OS2 algorithm is far less efficient than the two fourth order algorithms, *i.e.* the CGF4 and RQM4 algorithms, while the RQM4 algorithm is the most efficient one among them. Although all these three algorithms have the same computational complexity, they demand very different computation time to achieve the same accuracy for free energy calculations. Thus, the authors suggested that it is necessary to benchmark different competing algorithms rather than simply relying on their computational complexity to determine the actual performance they deliver. They also noticed that a proper selection of spatial and contour resolution, which balances the numerical inaccuracies, is critical to obtain optimum performance.

Here we present an alternative fourth-order algorithm based on an exponential time difference scheme (ETDRK4) to solve the MDEs. Following the suggestion of Stasiak and Matsen, we have performed a comprehensive benchmark among the OS2, RQM4 and the ETDRK4 algorithms, which shows our newly developed ETDRK4 algorithm is superior to the other two algorithms. The efficiency of the ETDRK4 algorithm is further demonstrated by applying it to compute several time-demanding complex structures: the O^{70} phase and the strong segregated bicontinuous gyroid phase.

NUMERICAL METHOD

Self-consistent Field Theory

The SCFT formulation of block copolymer melts is well established in the literature[5, 6], thus here we only list essential equations which are critical to introduce our numerical algorithms. Interesting readers are referred to the literature for more details.

We model n diblock copolymer chains composed of chemically incompatible components A and B in a volume V under the incompressible condition. The number of segments in a diblock copolymer chain is N and the volume fraction of A block is f. We assume A and B segments have the same length b and the same volume v_0. Thus, the density of the system is $\rho_0 = v_0^{-1}$. The Flory-Huggins interaction parameter between A and B segments is χ. In canonical ensemble, the mean-field free energy (in unit of k_BT) is given by

$$F / CV = -\frac{1}{V}\int \mathrm{d}\mathbf{r}\ \chi N\phi_A(\mathbf{r})\phi_B(\mathbf{r}) - \ln Q\left[\omega_A(\mathbf{r}), \omega_B(\mathbf{r})\right] \quad (1)$$

where $C = \rho_0 R_g^3 / N$ with $R_g = b\sqrt{N}/6$ being the radius of gyration of the diblock copolymer chain. Note that the spatial coordinate $\mathbf{r}$ is rescaled by R_g. The local density fields $\phi_A(\mathbf{r})$ and $\phi_B(\mathbf{r})$ and the auxiliary fields $\omega_A(\mathbf{r})$ and $\omega_B(\mathbf{r})$ at the saddle point are obtained by solving the following nonlinear equations in a self-consistent manner

$$\omega_A N = \chi N\phi_B + \xi N(\phi_A + \phi_B - 1) \quad (2a)$$

$$\omega_B N = \chi N\phi_A + \xi N(\phi_A + \phi_B - 1) \quad (2b)$$

$$\phi_A = \int_0^f \mathrm{d}s\ q(\mathbf{r}, s)q^*(\mathbf{r}, 1-s) \quad (2c)$$

$$\phi_B = \int_f^1 \mathrm{d}s\ q(\mathbf{r}, s)q^*(\mathbf{r}, 1-s) \quad (2d)$$

The auxiliary field $\xi(\mathbf{r})$ ensures the incompressible condition. The propagator $q(\mathbf{r}, s)$ describes the probability of finding a segment indexed by s at position $\mathbf{r}$ by propagating from the free end of A block. This propagator is the solution of the following modified diffusion equation (MDE)

$$\frac{\partial q(\mathbf{r}, s)}{\partial s} = \nabla^2 q - \omega q \quad (3)$$

subject to the initial condition $q(\mathbf{r}, 0) = 1$ and $\omega = \omega_A(\mathbf{r})$ for $s \in [0, f]$ and $\omega = \omega_B(\mathbf{r})$ for $s \in [f, 1]$. The backward propagator, $q^*(\mathbf{r}, s)$, initiated from the free end of B block also satisfies Eq. (3) subject to the initial condition $q^*(\mathbf{r}, 0) = 1$ and $\omega = \omega_B(\mathbf{r})$ for $s \in [0, 1-f]$ and $\omega = \omega_A(\mathbf{r})$ for $s \in [1-f, 1]$. The solution of the MDEs costs most of the computation time per SCFT iteration. It is critical to develop highly efficient algorithms for solving MDEs to improve the overall efficiency of the SCFT calculation. Below we describe our newly developed ETDRK4 algorithm as well as other two existing algorithms for solving Eq. (3). The single chain partition function Q in Eq. (1) can be evaluated as follows when the propagator is known

$$Q\left[\omega_A(\mathbf{r}), \omega_B(\mathbf{r})\right] = \frac{1}{V}\int \mathrm{d}\mathbf{r}\ q(\mathbf{r}, s = 1) \quad (4)$$

The integrals in Eqs. (1) and (4) are evaluated using a trapezoidal rule, which gives exponential accuracy because the integrands are periodic functions. The integrals in Eqs. (2c) and (2d) are evaluated using a Simpson's rule, which ensures the order of accuracy to be consistent with the ETDRK4 and RQM4 algorithms.

The ETDRK4 Algorithm

Recently, Liu and Zhang[22] developed a fourth-order exponential time differencing algorithm with Chebyshev

https://doi.org/10.1007/s10118-018-2037-7

collocation for solving SCFT equations of polymer brushes and confined polymers involving non-periodic boundary conditions. In this paper, we extend their work by modifying their ETDRK4 algorithm to accommodate periodic boundary conditions. Consequently, the modified ETDRK4 algorithm can be applied to bulk systems.

The original ETDRK4 algorithm was proposed by Cox and Matthews[23] and then improved by Kassam and Trefethen[24] to solve stiff nonlinear partial differential equations. First, we write the MDE in the following form

$$\frac{\partial q}{\partial s} = \mathcal{L}q + \mathcal{F}(q, s) \tag{5}$$

where $\mathcal{L} = \nabla^2$ and $\mathcal{F}(q, s) = -\omega(\mathbf{r})q$. A system of ordinary differential equations (ODEs) is then obtained by discretizing the spatial part of the MDE with $\mathbf{L}$ and $\mathbf{F}$ being the matrix representations for $\mathcal{L}$ and $\mathcal{F}$. The ODEs are solved by an exponential time difference (ETD) scheme which integrates over a single contour step from $s = s_n$ to $s = s_{n+1} + \Delta s$,

$$q(s_{n+1}) = \mathrm{e}^{\mathbf{L}\Delta s} q(s_n) + \mathrm{e}^{\mathbf{L}\Delta s} \int_0^{\Delta s} \mathrm{d}\tau\, \mathrm{e}^{\mathbf{L}\tau} \mathbf{F}(q(s_n + \tau), s_n + \tau) \tag{6}$$

In general, the integral in the above equation must be approximated to obtain the final algorithm. In this study, we adopt the fourth-order Runge-Kutta (RK) time stepping scheme proposed by Krogstad[25]. The set of equations for the scheme is listed below

$$a_n = \varphi_0(\mathbf{L}\Delta s/2)q_n + \frac{\Delta s}{2}\varphi_1(\mathbf{L}\Delta s/2)\mathbf{F}(q_n) \tag{7a}$$

$$b_n = a_n + \Delta s\varphi_2(\mathbf{L}\Delta s/2)\left[\mathbf{F}(a_n) - \mathbf{F}(q_n)\right] \tag{7b}$$

$$c_n = \varphi_0(\mathbf{L}\Delta s)q_n + \Delta s\varphi_1(\mathbf{L}\Delta s)\mathbf{F}(q_n) + 2\Delta s\varphi_2(\mathbf{L}\Delta s)\left[\mathbf{F}(b_n) - \mathbf{F}(q_n)\right] \tag{7c}$$

$$q_{n+1} = c_n + \Delta s\left[4\varphi_3(\mathbf{L}\Delta s) - \varphi_2(\mathbf{L}\Delta s)\right]\left[\mathbf{F}(q_n) + \mathbf{F}(c_n)\right] + 2\Delta s\varphi_2(\mathbf{L}\Delta s)\mathbf{F}(a_n) - 4\Delta s\varphi_3(\mathbf{L}\Delta s)[\mathbf{F}(a_n) + \mathbf{F}(b_n)] \tag{7d}$$

The coefficients in above equations are defined as $\varphi_{l+1}(z) = [\varphi_l(z) - 1/l!]/z$ with $l = 0, 1, 2$ and $\varphi_0(z) = \exp(z)$. It should be noted that serious cancellation errors emerge when one tries to evaluate the coefficients directly. Similar to the approach described in detail in Ref. [21], we employ the technique based on complex contour integral proposed by Kassam and Trefethen[24] to circumvent this difficulty.

For periodic boundary condition problems, the matrix $\mathbf{L}$ can be diagonalized by transforming the MDE into the Fourier space, which greatly simplifies the calculation. After the Fourier transformation, the matrix $\mathbf{L}$ reduces to $-R_g\mathbf{k}^2\mathbf{I}$, and $\mathbf{F}(q) = -\widehat{\omega q}(\mathbf{k})\mathbf{I}$, where $\mathbf{I}$ is an identity matrix, $\mathbf{k}$ is a wave vector in Fourier space, and $\widehat{\omega q}(\mathbf{k})$ denotes the Fourier transform of the function $\omega(\mathbf{r})q(\mathbf{r})$. Note that $\widehat{\omega q}(\mathbf{k})$ should be transformed back to real space to evaluate the nonlinear term after each time stepping.

The OS2 Algorithm

Rasmussen and Kalosakas[17] adopted an operator splitting method to separate the MDE into a diffusive term and a potential term[5, 17, 19]

$$q(\mathbf{r}, s + \Delta s) = \exp[\mathcal{L}^W \Delta s/2]\exp[\mathcal{L}^D \Delta s]\exp[\mathcal{L}^W \Delta s/2]q(\mathbf{r}, s) + O(\Delta s^3) \tag{8}$$

where $\mathcal{L}^D = \nabla^2$ and $\mathcal{L}^W = -w(\mathbf{r})$. This approach results in a second-order accurate algorithm. The operation counts for executing this algorithm for a single contour step Δs is $O(M\log_2 M)$ with M the total number of collocation points (*i.e.* number of plane waves). By repeating the procedure along the chain contour, the solution of the diffusion equation requires $O(N_s M\log_2 M)$ with $N_s = \Delta s^{-1}$ being the total number of contour steps.

The RQM4 Algorithm

The RQM4 algorithm was developed by simply carrying out a Richardson extrapolation on the OS2 algorithm[19]. Propagators $q_{\Delta s}(\mathbf{r}, s)$ and $q_{\Delta s/2}(\mathbf{r}, s)$ are first obtained by solving the MDE using the OS2 algorithm with contour steps of Δs and $\Delta s/2$, respectively. Then they are combined in the following way to give the final solution of the propagator

$$q(\mathbf{r}, s) = [4q_{\Delta s/2}(\mathbf{r}, s) - q_{\Delta s}(\mathbf{r}, s)]/3 \tag{9}$$

This algorithm possesses a fourth-order accuracy for contour stepping owing to the fact that the errors of $q_{\Delta s}(\mathbf{r}, s)$ and $q_{\Delta s/2}(\mathbf{r}, s)$ cancel out exactly to the fourth-order.

RESULTS AND DISCUSSION

Performance of the ETDRK4 Algorithm

Convergence in N_s

In this part, we investigate the performance of the ETDRK4 algorithm and compare it with the OS2 algorithm[17] and the RQM4 algorithm[19]. In particular, the dependence of the accuracy of the SCFT calculation on the number of contour steps N_s, which defines the contour resolution, has been examined. For all benchmark runs, we choose a diblock copolymer melt with the volume fraction of A block $f = 0.375$ at $\chi N = 18$. Such a melt is known to form a bicontinuous gyroid structure[15, 26]. All simulations are performed in a cubic unit cell with a stress-free cell size and are initialized by a gyroid structure obtained from a SCFT calculation of a diblock copolymer melt of $f = 0.37$ and $\chi N = 18$ with $N_s = 100$ and $M = 32^3$. For all simulations, the spatial resolution is fixed at $M = 32^3$.

We use the numerical error of the mean-field free energy F to measure the accuracy of various algorithms[18, 19, 21]. The numerical error is defined as $e(N_s) = F(N_s) - F_0$, where $F(N_s)$ is the free energy computed by the SCFT calculation and F_0 is the exact solution. Unfortunately, in general the exact value of F_0 is not available. A conventional approach to circumvent this difficulty is taking the mean-field free energy computed by SCFT with the highest possible contour and spatial resolution as F_0. However, this approach introduces extra numerical errors associated with the so-computed F_0. Moreover, the computation of F_0 costs a significant amount of the computation time during benchmark since a dramatically high resolution is required to obtain reasonably accurate F_0. Here, we propose an alternative approach to avoid computing F_0 by defining a "relative error" $\Delta e = e(N_s) - e(N_s') = F(N_s) - F(N_s') = \Delta F$ where N_s' is the number of contour steps of the

https://doi.org/10.1007/s10118-018-2037-7

adjacent benchmark run to N_s and $N_s > N_s'$. It can be shown[27] that ΔF is related to the numerical error as $\Delta F = (r^p - 1)e$, where r is the ratio of the size of contour step on the coarse grid to that on the fine grid, and p is the theoretical order of accuracy. By properly choosing the contour steps for each benchmark simulations, $r^p - 1$ can be restricted to a small range around 1. Therefore, ΔF should be a good estimate of e, allowing us to use ΔF directly in the following benchmark.

We have carried out a series of benchmark runs with various number of contour steps and plotted the relative error as a function of N_s in Fig. 1(a). In this log-log plot, the slope of a curve for an algorithm indicates the order of accuracy of this algorithm. It clearly shows that the OS2 algorithm is second-order accurate as expected, while our ETDRK4 algorithm possesses the same order of accuracy as the RQM4 algorithm which is fourth-order. Remarkably, it can be seen that the whole curve of the ETDRK4 algorithm is below the curve of the RQM4 algorithm. The difference of the relative error between these two algorithms is more than one order of magnitude. It means that, at the same contour resolution, our ETDRK4 algorithm is at least ten times more accurate than the RQM4 algorithm. Consequently, we can use much fewer contour steps in the ETDRK4 algorithm to obtain the same level of accuracy as the RQM4 algorithm.

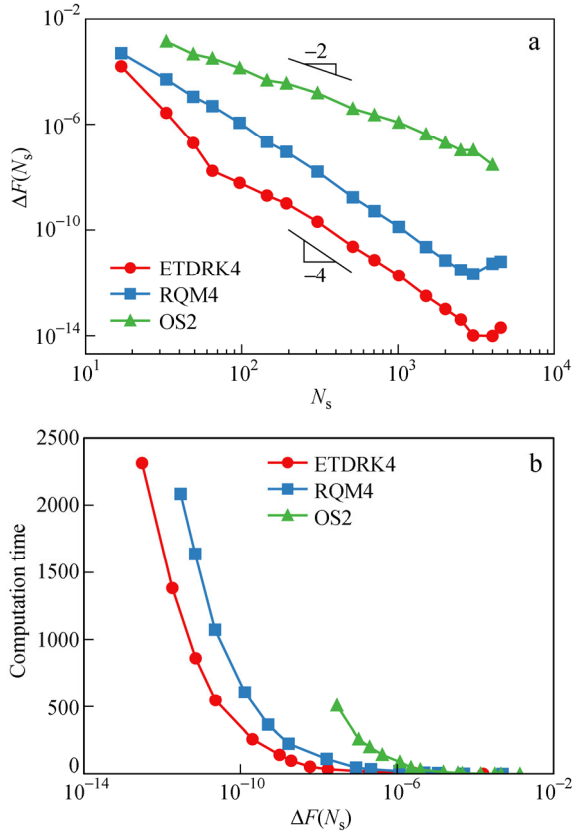

Fig. 1 Performance of the ETDRK4, RQM4 and OS2 algorithms in computing the bicontinuous gyroid structure of a AB diblock copolymer melt with $f = 0.375$ and $\chi N = 18$: (a) the relative error as a function of N_s and (b) the least total computation time needed to achieve the relative error $\Delta F(N_s)$ (The spatial resolution is fixed at $M = 32^3$)

The order of accuracy alone, however, cannot fully characterize the performance of an algorithm. The efficiency of an algorithm also depends on the number of operations for each contour stepping. Although our ETDRK4 algorithm outperforms other two algorithms in the aspect of accuracy at the same contour resolution as shown in Fig. 1(a), it is not necessarily true to conclude that the ETDRK4 algorithm is the fastest one to achieve a certain level of accuracy because for each contour stepping it requires four pairs of FFT operations which are larger than one and two pairs for the OS2 algorithm and the RQM4 algorithm, respectively. In fact, a more complete way to compare the efficiency of different algorithms is to compare their overall computation time for obtaining a certain level of accuracy. The computation time as a function of $\Delta F(N_s)$ is thus plotted in Fig. 1(b). It clearly shows that our ETDRK4 algorithm requires much less computation time than the RQM4 algorithm to obtain a certain level of accuracy. Moreover, the advantage of the ETDRK4 algorithm expands as the given accuracy increases.

Convergence in N_x

In this part, we examine the convergence property in the spatial domain of the ETDRK4, OS2 and RQM4 algorithms. A series of SCFT calculations have been performed with various spatial resolution at fixed contour resolution. A diblock copolymer melt with $f = 0.32$ is chosen, which also forms a bicontinuous gyroid phase at $\chi N = 40$. Similar to the previous part, all simulations are performed in a cubic unit cell with a stress-free cell size. The spatial resolution is determined by the number of collocation points along each direction in the unit cell which is denoted as N_x. Note that the total number of collocation points in a unit cell is $M = N_x^3$.

We adopt the relative error approach introduced in the previous part to characterize the accuracy of various algorithms. The relative errors of various algorithms as a function of the spatial resolution are plotted in Fig. 2. The three algorithms are all pseudo-spectral algorithms. It is expected that they should converge exponentially in the spatial resolution. For the same segregation strength of $\chi N = 40$, it can be seen that the curves of three algorithms almost

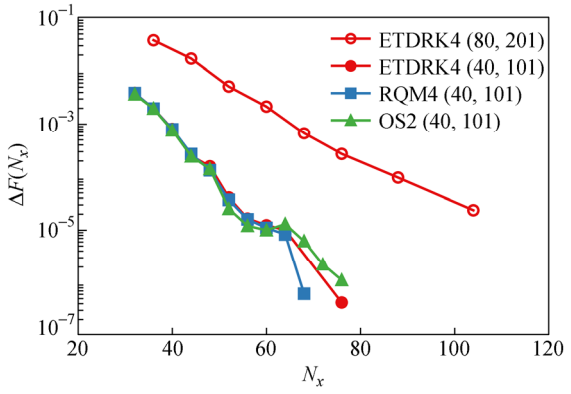

Fig. 2 Convergence property in the spatial resolution of various algorithms for computing bicontinuous gyroid structure of a diblock copolymer melt with $f = 0.32$ ($\Delta F(N_x)$ is a relative error defined as the difference of the free energies between two adjacent SCFT simulations. The numbers in the parentheses in the legend denote the values of χN and N_s, respectively.)

https://doi.org/10.1007/s10118-018-2037-7

coincide with each other, indicating that they share the same convergence rate. Moreover, they all converge exponentially, *i.e.* decaying linearly in the semilog plot shown in Fig. 2, as expected. For stronger segregation strength (χN = 80), the exponential convergence rate of the ETDRK4 algorithm does not change. However, its accuracy degrades significantly due to the increase of the segregation strength. The decrease of accuracy can be understood that the interface between A-rich and B-rich domains becomes sharper as the segregation strength increases which requires higher spatial resolution to compute it accurately. Therefore, it becomes harder and harder to compute the gyroid structure when the segregation strength enhances. This provides a good opportunity to further address the performance of various algorithms which we will discuss in the next section.

Application 1: Phase Boundaries of the Gyroid Phase in the Strong Segregation Regime

The bicontinuous gyroid phase has once been mistakenly identified as the ordered bicontinuous double diamond (OBDD) phase in the experiments[28]. Later, Matsen and Schick[15] proved that the gyroid phase is actually more stable in the weak and intermediate segregation regime based on SCFT calculations using the spectral algorithm. However, in the strong segregation regime a triple point at around $\chi N = 60$ was inferred from their SCFT calculations and above it the gyroid phase lost its stability[29], reflecting the difficulty of using the fully spectral algorithm in dealing with the self-assembly of block copolymers in strong segregation regime where a large number of basis functions are needed. Cochran, Garcia-Cervera and Fredrickson[18] readdressed this issue using a more efficient fourth-order pseudo-spectral algorithm (CGF4). No evidence of the loss of stability of the gyroid structure has been found by computing at segregation strength up to 100.

The performance of three pseudo-spectral algorithms, the OS2 algorithm, the CGF4 algorithm and the RQM4 algorithm, as well as the full spectral algorithm has been systematically studied by Stasiak and Matsen for the SCFT calculations of the gyroid phase in the weak and intermediate segregation regime[21, 30]. It is found that the most efficient algorithm is the full spectral algorithm when the segregation strength is weak ($\chi N < 40$). However, the efficiency of the full spectral algorithm decreases sharply with the increase of segregation strength due to its $O(M^3)$ computational complexity, which renders it of little use in the strong segregation regime ($\chi N >$ 50). In the strong segregation regime, the RQM4 algorithm delivers the best performance among all the algorithms they have tested.

We have demonstrated in the previous section that our ETDRK4 algorithm performs better than the RQM4 algorithm when the segregation strength is 18 (weak segregation). Here we further compare the performance of these two algorithms in strong segregation regime and investigate the dependence of the efficiency on the segregation strength. We first analyze the order of accuracy of these two algorithms as a function of the segregation strength as shown in Fig. 3(a). It can be seen that the order of accuracy of our ETDRK4 algorithm is slightly better than the expected fourth-order. Furthermore, the order of accuracy even improves as the segregation strength increases. On the contrary, the order of accuracy of the RQM4 algorithm gradually decreases and it is worse than that of the ETDRK4 algorithm for all χN values we have tested. This discrepancy suggests that we can use fewer contour steps in our ETDRK4 algorithm as compared to the RQM4 algorithm, which is confirmed by plotting the optimum number of contour steps for both algorithms to ensure the relative error less than 10^{-4} as a function of χN in Fig. 3(b). Figure 3(c) displays the total computation time to solve a MDE for both algorithms, which further confirms the previous conclusion. Note that the ETDRK4 is about 30% faster than the RQM4 algorithm at $\chi N = 80$.

It is helpful to break down the total computation time for solving a MDE into two factors: the number of contour steps and the computation time per contour step. The ratios of these two factors between the ETDRK4 and the RQM4 algorithms are plotted in Fig. 3(d). It reveals that although the ETDRK4 algorithm is about 1.5 times slower than the RQM4 algorithm for computing each contour step, the RQM4 algorithm requires at least 1.7 times more contour steps, resulting in the better performance of the ETDRK4 algorithm. Moreover, the ratio of the computation time per contour step remains constant while the ratio of the number of contour steps amplifies as χN increases. Therefore, the improvement of our ETDRK4 algorithm mainly comes from the efficient reduction of the number of contour steps.

With our improved algorithm, we now are ready to apply it to solve real problems and check its practical performance. In particular, here we utilized it to determine phase boundary points on the cylindrical/gyroid (C/G) phase boundary and the gyroid/lamellar (G/L) phase boundary at $\chi N = 40$ and $\chi N = 80$. The precision of the phase boundary point depends on the accuracy of the computed free energy. To obtain four significant digits of $f_{C/G}$ and $f_{G/L}$, we need the spatial and the contour resolution high enough that the error of the free energy is less than 10^{-5}. For $\chi N = 40$, this requires $N_s \approx 100$ contour points and $N_x \approx 64$ collocation points for each dimension of the unit cell. These values can be obtained by looking them up in Figs. 1(a) and 2. Similarly, at $\chi N = 80$, it requires $N_s \approx 150$ and $N_x \approx 128$. The results are shown in Table 1 where we also list previously reported phase boundary points computed by the CGF4 algorithm and the full spectral algorithm for comparison[18, 30]. As can be seen, the ETDRK4 algorithm is significantly better than the CGF4 algorithm since the CGF4 algorithm with $N_s \approx 1000$ and $N_x \approx 128$ only gives three significant digits. Note that our results are almost identical to those obtained by the full spectral algorithm with 5000 basis functions. It is difficult to directly compare our algorithm with the spectral algorithm since the efficiency of these two algorithms is controlled by different parameters. However, the poor computational complexity $O(M^3)$ of the spectral algorithm implies that our algorithm should do better when χN is large enough owing to the fact that our algorithm only scales as $N_s M \ln M$.

https://doi.org/10.1007/s10118-018-2037-7

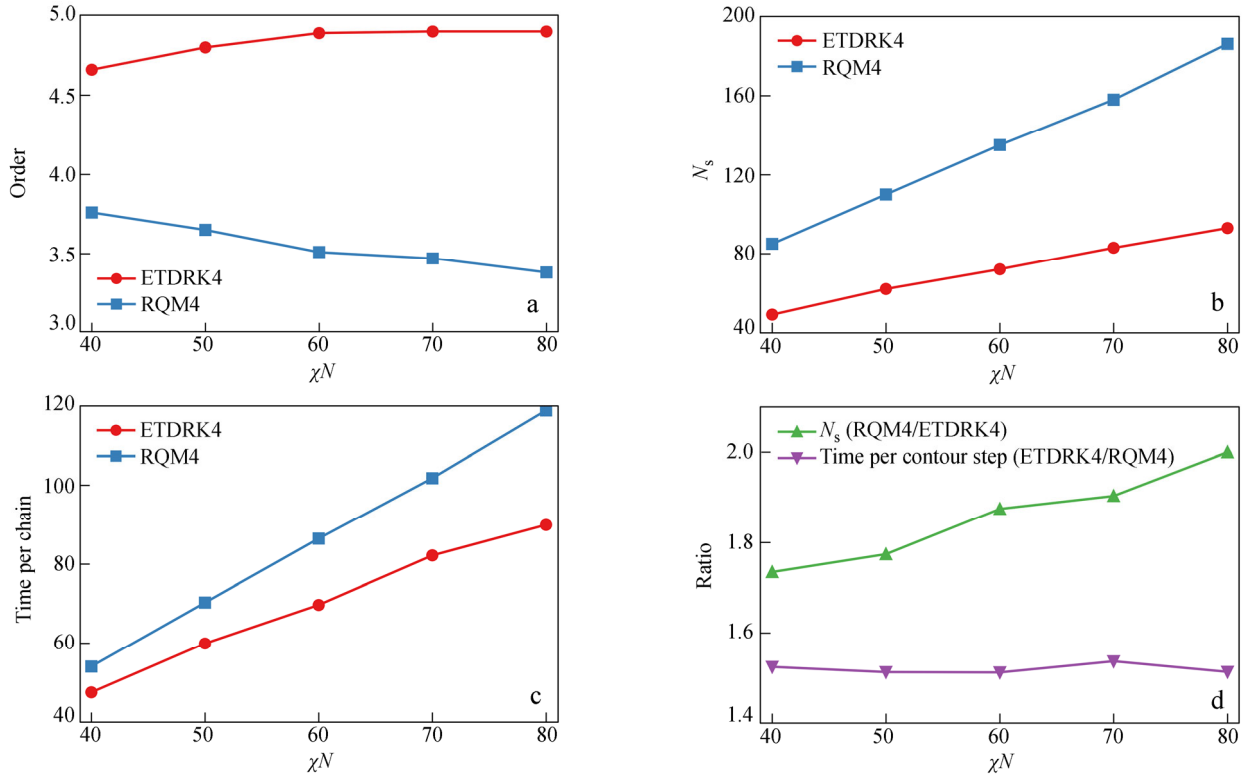

Fig. 3 Comparison of the performance of the ETDRK4 and RQM4 algorithms in computing the gyroid structure of the diblock copolymer melt in strong segregation regime: (a) the order of accuracy as a function of χN, (b) the optimum N_s to ensure the relative error $\Delta F(N_s)$ is less than 10^{-4} as a function of χN, (c) the total computation time to solve a MDE as a function of χN, (d) the ratio of the optimum N_s needed by the RQM4 algorithm to that needed by the ETDRK4 algorithm, and the ratio of computation time per contour step of the ETDRK4 algorithm to that of the RQM4 algorithm (The spatial resolution is fixed at $N_x = 128$.)

Table 1 Phase boundary points of the gyroid phase as a function of the segregation strength

χN	$f_{C/G}$			$f_{G/L}$			$\Delta f = f_{G/L} - f_{C/G}$		
	ETDRK4	CGF4[18]	Spectral[30]	ETDRK4	CGF4	Spectral	ETDRK4	CGF4	Spectral
40	0.3152_5	0.315_3	0.31528	0.3374_1	0.336_7	0.33742	0.0221_6	0.021_7	0.02214
80	0.3096_6	0.308_8	0.3096	0.3242_6	0.324_2	0.3244	0.0145_9	0.015_4	0.0148

$f_{C/G}$ and $f_{L/G}$ are the volume fraction of the A block at the C/G phase boundary and the L/G phase boundary, respectively, and Δf is the width of the gyroid phase region.

Application 2: Triple Point of C/L/O^{70}

Bates and coworkers[31, 32] discovered an interesting noncubic triply periodic network structure (O^{70}) in linear triblock copolymer melts, which is topologically similar to the gyroid phase and the hexagonally perforated lamellar (HPL) phase[31]. Using SCFT calculations, Tyler and Morse[33] predicted that the O^{70} phase is also stable in diblock copolymer melts in addition to linear triblock copolymer melts. For the diblock copolymer melts, the O^{70} phase appears in the weak segregation regime and is enclosed by the L, G, and C phases. There are two obvious triple points, L/G/O^{70} and C/G/O^{70}, which have been first calculated by Tyler and Morse[33] and later refined by Matsen[30]. However, it remains unclear about the existence of the C/L/O^{70} triple point due to the limitation of numerical accuracy of previous SCFT calculations[33].

In this study, our improved algorithm empowers us to extend the work of Matsen[30] to explore the C/L/O^{70} triple point. Figure 4 illustrates two possible scenarios of the phase diagram near the critical point. The metastable C/L phase boundary, where $F_C = F_L$, should locate inside the O^{70} phase region[30]. If the C/L/O^{70} triple point does not exist, the metastable C/L phase boundary will extend to the critical point. Otherwise, it will end at the C/L/O^{70} triple point and the stable C/L phase boundary connects the triple point and the critical point. To confirm the existence of this triple point, it is most convenient to compute the free energy of the O^{70} phase and compare it with the metastable C/L phase boundary.

The metastable C/L phase boundary can be determined by sweeping χN at each given f. Some typical sweeps are shown in Fig. 5(a) by plotting $F_C - F_L$ as a function of χN. Clearly, the crossover point between the data curve and the $F_C - F_L = 0$ line is the phase boundary point. The metastable C/L phase boundary is then obtained by connecting all these crossover points as shown in Fig. 5(b). The rightmost point on the phase boundary computed by the ETDRK4 algorithm, *i.e.* the one closest to the critical point, is ($f = 0.499$, $\chi N = 10.49514$). Note that the critical point is ($f = 0.5$, $\chi N = 10.495$).

https://doi.org/10.1007/s10118-018-2037-7

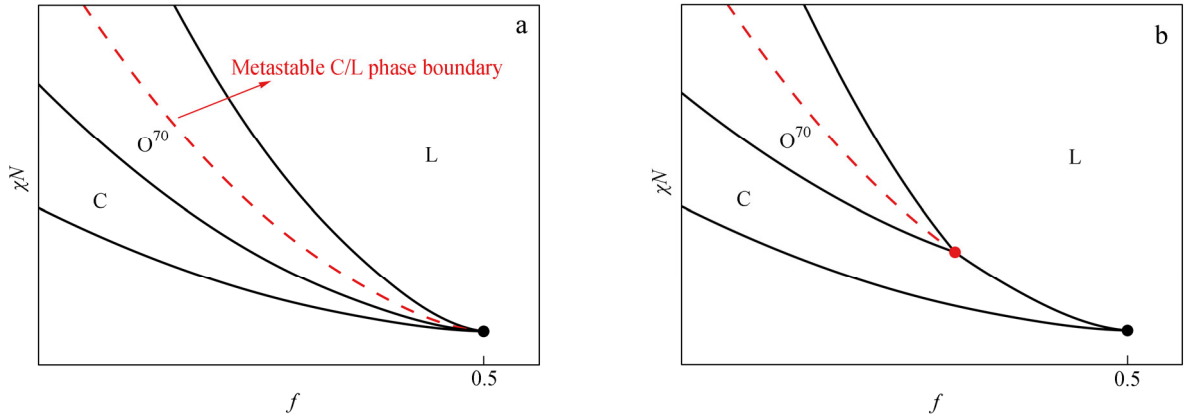

Fig. 4 Illustration of the possible topology of the metastable C/L phase boundary inside the O^{70} phase region (a) if the C/L/O^{70} triple point does not exist or (b) if it exists (The black dot at $f = 0.5$ is the critical point)

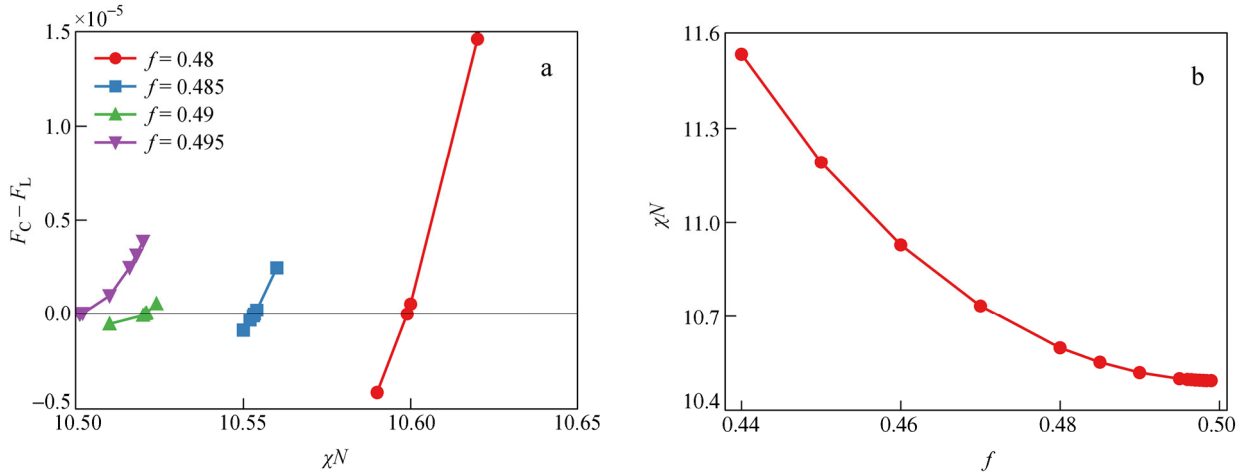

Fig. 5 (a) Determination of the metastable C/L phase boundary by identifying crossover points where $F_C - F_L = 0$; (b) The metastable C/L phase boundary for a diblock copolymer melt

To see whether the O^{70} phase changes its stability along the metastable C/L phase boundary, it is helpful to plot the free energy difference $F_{C/L} - F_{O^{70}}$ in Fig. 6. It can be seen that the free energy difference is always positive, meaning that the O^{70} phase is stable all along the metastable C/L phase boundary we have calculated. Therefore, it appears that the C/L/O^{70} triple point does not exist when $f \leq 0.499$. Note that the difference of the free energy at $f = 0.499$ is extremely small (about 10^{-11}). And it will become even smaller when f approaches 0.5, which makes the numerical calculation infeasible. However, it seems that the trend of the decrease of the free energy difference will continue and the curve will eventually converge at the critical point, suggesting that the C/L/O^{70} triple point does not exist corresponding to the scenario of Fig. 4(b). On the other hand, even if the C/L/O^{70} triple point does exist in the range of $0.499 < f < 0.5$, in practical it is not that important because it is almost impossible to control the volume fraction of the A block in such a narrow range. Moreover, the phase diagram near the critical point is vulnerable to thermal fluctuations and the C/L/O^{70} triple point will be destroyed under the experimental condition.

It is worth explaining why it is difficult to address the

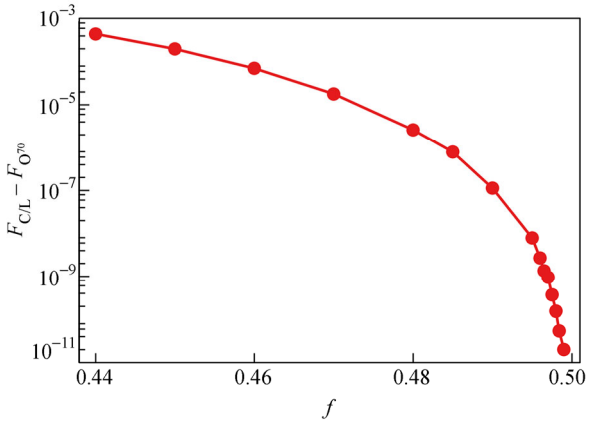

Fig. 6 The difference of the free energy between the C/L meta boundary and the O^{70} phase, $F_{C/L} - F_{O^{70}}$, as a function of the volume fraction of the A block

stability of the O^{70} phase close to the critical point. There are mainly two reasons. One is that the extremely small free energy difference requires the same level of accuracy of the free energy which in turn requires significantly high spatial and contour resolution in SCFT calculations. In principle,

https://doi.org/10.1007/s10118-018-2037-7

the best accuracy one can achieve is the machine accuracy which is about 10^{-16} for double precision floating point calculations. In practice, however, the best accuracy is limited by other factors such as the rounding error and the mismatch of the spatial and contour resolution. For a typical implementation of the ETDRK4 algorithm, the limit of the accuracy is about 10^{-14}.

The other reason is best explained by Fig. 7. The free energy of a phase should be computed with a stress-free unit cell size. This size can be obtained by adjusting the cell size to minimize the free energy. Figure 7(a) shows a typical minimization for the O^{70} phase with $f = 0.495$ at $\chi N = 10.5012$ using the Brent method[34]. The stress-free size L^* corresponds to the minimum position which is $3.7298R_g$ in this case. As the cell size deviates from the stress-free size by $\Delta L = L - L^*$, the free energy increases from $F(L^*)$ to $F(L)$. Therefore, it introduces an extra error $\Delta F = F(L^*) - F(L)$ to the free energy, which scales as ΔL^2 as revealed by the log-log plot in Fig. 7(b). The error ΔF can be reduced by carrying out more minimizing iterations. However, it requires enormous number of iterations to reduce ΔF down to the level of 10^{-12}, which makes the calculation infeasible.

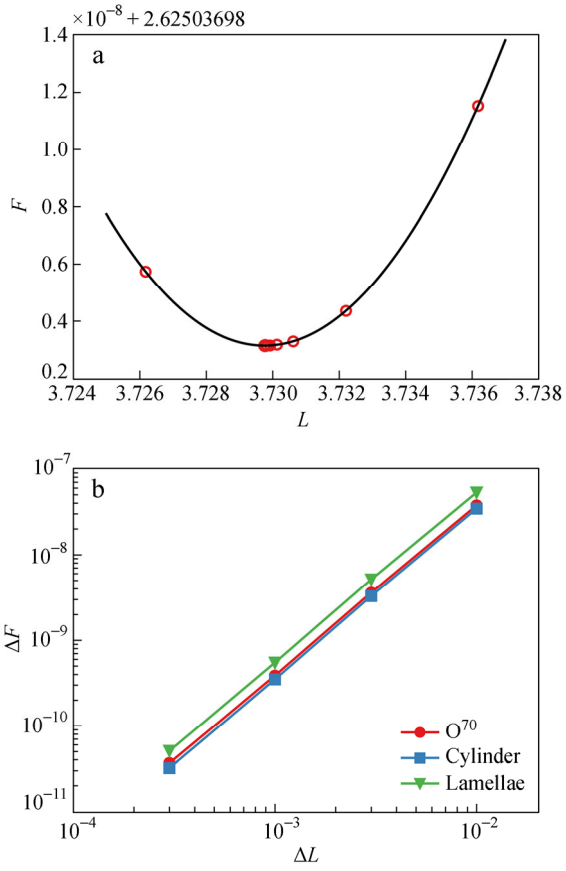

Fig. 7 Influence of the unit cell size on the free energy of a diblock copolymer melt with $f = 0.495$ at $\chi N = 10.5012$: (a) the free energy of the O^{70} phase as a function of the unit cell size in the vicinity of the stress-free size ($L^* = 3.7298R_g$) corresponding to the minimum free energy; (b) deviation of the free energy from the minimum, $\Delta F = F(L) - F(L^*)$, as a function of $\Delta L = L - L^*$ (The solid curve in (a) is a parabola which best fits the data.)

CONCLUSIONS

A fourth-order exponential time differencing Runge-Kutta algorithm has been developed to solve the modified diffusion equation, which greatly improves the efficiency of the SCFT calculation. According to our benchmark, it is the convergence property in the chain contour resolution that makes the ETDRK4 algorithm superior to other algorithms such as OS2, CGF4, and RQM4. The superior performance of the ETDRK4 algorithm is also owing to the fact that it converges exponentially in the spatial resolution, which is the best convergence rate a numerical algorithm can achieve.

The power of our improved algorithm has been demonstrated by applying it to calculate two representative examples in diblock copolymer melts: the bicontinuous gyroid phase in the strong segregation regime and the stability of the O^{70} phase close to the critical point. The calculation of the gyroid phase in the strong segregation regime requires tremendous computational resources using existing algorithms. With our ETDRK4 algorithm, it is possible to significantly reduce the computational cost. More remarkably, the performance of the ETDRK4 algorithm becomes better as the segregation strength enhances, while on the contrary the RQM4 algorithm, as the most efficient algorithm among all reported algorithms, gets worse. This makes our ETDRK4 algorithm the best choice for calculating strongly segregated systems. Apart from the accuracy of the ETDRK4 algorithm, its correctness was also verified by computing the C/G and G/L phase boundary points at $\chi N = 40$ and $\chi N = 80$ and comparing them with those computed by the full spectral algorithm.

Another challenging problem is to examine the existence of the C/L/O^{70} triple point in diblock copolymer melts. The major difficulty is that the free energy difference between the metastable C/L phase boundary and the O^{70} phase close to the critical point becomes extremely tiny. Using our ETDRK4 algorithm, we have verified that there is no C/L/O^{70} triple point up to $f = 0.499$. It becomes infeasible to further improve our result because we have hit the machine accuracy using double precision floating arithmetic. However, the trend of the change of the free energy difference towards the critical point highly suggests that the C/L/O^{70} triple point does not exist. As the most efficient real-space technique to date, we expect that the ETDRK4 algorithm will become the first choice for high accuracy SCFT calculations of complex phase microstructures of block copolymers in the near future.

ACKNOWLEDGMENTS

This work was financially supported by the China Scholarship Council (No. 201406105018), the National Natural Science Foundation of China (No. 21004013) and the National Basic Research Program of China (No. 2011CB605701).

REFERENCES

1 Edwards, S. F. Statistical mechanics of polymer with excluded volume. Proc. Phys. Soc. London 1965, 85 (546P), 613–624.
2 de Gennes, P. G. "Scaling concepts in polymer physics", Cornell University Press, Ithaca 1969.

3 Helfand, E. Block copolymer theory. 3. Statistical-mechanics of microdomain structure. Macromolecules 1975, 8(4), 552–556.
4 Hong, K. M.; Noolandi, J. Theory of inhomogeneous multicomponent polymer systems. Macromolecules 1981, 14(3), 727–736.
5 Fredrickson, G. H. "The equilibrium theory of inhomogeneous polymers", Oxford University Press, New York 2006.
6 Matsen, M. W. Undulation instability in block-copolymer lamellae subjected to a perpendicular electric field. Soft Matter 2006, 2(12), 1048–1056.
7 Bates, F. S.; Hillmyer, M. A.; Lodge, T. P.; Bates, C. M.; Delaney, K. T.; Fredrickson, G. H. Multiblock polymers: panacea or pandora's box? Science 2012, 336(6080), 434–440.
8 Matsen, M. W.; Thompson, R. B. Equilibrium behavior of symmetric ABA triblock copolymer melts. J. Chem. Phys. 1999, 111(15), 7139–7146.
9 Tang, P.; Qiu, F.; Zhang, H. D.; Yang, Y. L. Morphology and phase diagram of complex block copolymers: ABC star triblock copolymers. J. Phys. Chem. B 2004, 108(24), 8434–8438.
10 Xie, N.; Liu, M. J.; Deng, H. L.; Li, W. H.; Qiu, F.; Shi, A. C. Macromolecular metallurgy of binary mesocrystals *via* designed multiblock terpolymers. J. Am. Chem. Soc. 2014, 136(8), 2974–2977.
11 Duchs, D.; Sullivan, D. E. Entropy-induced smectic phases in rod-coil copolymers. J. Phys. Condens. Matter 2002, 14(46), 12189–12202.
12 Matsen, M. W. Thin films of block copolymer. J. Chem. Phys. 1997, 106(18), 7781–7791.
13 Leibler, L. Theory of microphase separation in block co-polymers. Macromolecules 1980, 13(6), 1602–1617.
14 Semenov, A. N. Contribution to the theory of microphase layering in block-copolymer melts. Zh. Eksp. Teor. Fiz. 1985, 88(4), 1242–1256.
15 Matsen, M. W.; Schick, M. Stable and unstable phases of a diblock copolymer melt. Phys. Rev. Lett. 1994, 72(16), 2660–2663.
16 Drolet, F.; Fredrickson, G. H. Combinatorial screening of complex block copolymer assembly with self-consistent field theory. Phys. Rev. Lett. 1999, 83(21), 4317–4320.
17 Rasmussen, K. O.; Kalosakas, G. Improved numerical algorithm for exploring block copolymer mesophases. J. Polym. Sci., Part B: Polym. Phys. 2002, 40(16), 1777–1783.
18 Cochran, E. W.; Garcia-Cervera, C. J.; Fredrickson, G. H. Stability of the gyroid phase in diblock copolymers at strong segregation. Macromolecules 2006, 39(7), 2449–2451.
19 Ranjan, A.; Qin, J.; Morse, D. C. Linear response and stability of ordered phases of block copolymer melts. Macromolecules 2008, 41(3), 942–954.
20 Tong, C. H.; Zhu, Y. J.; Zhang, H. D.; Qiu, F.; Tang, P.; Yang, Y. L. The self-consistent field study of the adsorption of flexible polyelectrolytes onto two charged nano-objects. J. Phys. Chem. B 2011, 115(39), 11307–11317.
21 Stasiak, P.; Matsen, M. W. Efficiency of pseudo-spectral algorithms with Anderson mixing for the SCFT of periodic block-copolymer phases. Eur. Phys. J. E 2011, 34(10), 110.
22 Liu, Y. X.; Zhang, H. D. Exponential time differencing methods with Chebyshev collocation for polymers confined by interacting surfaces. J. Chem. Phys. 2014, 140(22), 224101.
23 Cox, S. M.; Matthews, P. C. Exponential time differencing for stiff systems. J. Comput. Phys. 2002, 176(2), 430–455.
24 Kassam, A. K.; Trefethen, L. N. Fourth-order time-stepping for stiff PDEs. SIAM J. Sci. Comput., 2005, 26(4), 1214–1233
25 Krogstad, S. "Topics in numerical Lie group integration", Ph.D. thesis, The University of Bergen, 2003.
26 Matsen, M. W.; Bates, F. S. Block copolymer microstructures in the intermediate-segregation regime. J. Chem. Phys. 1997, 106(6), 2436–2448.
27 Oberkampf, W. L.; Roy, C. J. "Verification and validation for scientific computing", Cambridge University Press, New York, 2010.
28 Thomas, E. L.; Alward, D. B.; Kinning, D. J.; Martin, D. C.; Handlin, D. L.; Fetters, L. J. Ordered bicontinuous doublediamond structure of star block copolymers-a new equilibrium microdomain morphology. Macromolecules 1986, 19(8), 2197–2202.
29 Matsen, M. W.; Bates, F. S. Origins of complex self-assembly in block copolymers. Macromolecules 1996, 29(23), 7641–7644.
30 Matsen, M. W. Fast and accurate SCFT calculations for periodic block-copolymer morphologies using the spectral method with Anderson mixing. Eur. Phys. J. E, 2009, 30(4), 361–369.
31 Epps, T. H.; Cochran, E. W.; Bailey, T. S.; Waletzko, R. S.; Hardy, C. M.; Bates, F. S. Ordered network phases in linear poly(isoprene-*b*-styrene-*b*-ethylene oxide) triblock copolymers. Macromolecules 2004, 37(22), 8325–8341.
32 Bailey, T. S.; Hardy, C. M.; Epps, T. H.; Bates, F. S. A noncubic triply periodic network morphology in poly(isoprene-*b*-styrene-*b*-ethylene oxide) triblock copolymers. Macromolecules 2002, 35(18), 7007–7017.
33 Tyler, C. A.; Morse, D. C. Orthorhombic Fddd network in triblock and diblock copolymer melts. Phys. Rev. Lett. 2005, 94(20), 208302.
34 Press, W. H., Teukolsky, S. A. Vetterling, W. T. and Flannery, B. P., "Numerical recipes 3rd edition: The art of scientific computing", Cambridge University Press, New York 2007.

https://doi.org/10.1007/s10118-018-2037-7